Chapter 8

GEL FORMATION: PHASE DIAGRAMS USING TABLETOP RHEOLOGY AND CALORIMETRY

Srinivasa R. Raghavan and Bani H. Cipriano
Department of Chemical Engineering, University of Maryland, College Park, MD 20742

1. Introduction

In previous chapters, we have attempted to define the term "gel" in a consistent and meaningful way, while recognizing that the gel state is often easier to recognize than to define (if it looks like "Jello", feels like "Jello", and responds like "Jello", it must be a gel [1]). This leads us to the theme of the present chapter, the elucidation of phase diagrams and composition maps for molecular gels. Typically, this is the first step in a given study. Other chapters are devoted to detailed analyses of gels and their phase transitions (see Chapters 1–4).

It is worthwhile to recall that molecular gel samples are usually prepared by dissolving a small-molecule gelator in a liquid, usually by warming [1]. At this point, the gelator is unaggregated or in small aggregates and this system is referred to as a *sol*. The sol is then cooled below a transition temperature whereupon it transforms into a *gel*. Typically, the higher the gelator concentration c, the higher is the *sol-gel* transition temperature T_{gel} and a plot of T_{gel} against c constitutes a phase boundary. A phase diagram is a map of T vs. c showing the sol-gel boundaries as well as the boundaries of any multi-phase or lyotropic liquid crystal regions that are also present. Most articles on molecular gels usually have an accompanying phase diagram.

While studying gelators, especially those with novel structures, the focus is on determining the entire phase diagram rapidly and using as little gelator as is practically feasible. Thus, there is a need for simple, reliable, and

R.G. Weiss and P. Terech (eds.),
Molecular Gels: Materials with Self-Assembled Fibrillar Networks, 233–244.
© 2005 *Springer. Printed in the Netherlands.*

convenient techniques for phase characterization. Two such techniques fit the bill and are widely used by practitioners for a broad range of molecular gelators:

(1) **"Tabletop" rheological techniques**: These are techniques such as the tube inversion and falling sphere methods that have a rheological basis. More detailed analyses of rheological properties of gels are found in Chapters 5 and 6.
(2) **Thermal characterization methods**: In particular, differential scanning calorimetry (DSC).

We will now consider these two techniques systematically in the rest of this chapter. A variety of other techniques that are useful in studying specific types of gelators are discussed in Chapters 9–13.

2. Detecting the Sol-Gel Transition by Tabletop Rheology

The definitive signature of a gel is its elastic rheological response, or more precisely, the presence of a *non-zero equilibrium modulus* G_e [2]. There are two alternative ways of stating the same idea: the gel should *not relax* under a small mechanical stress even if given an infinitely long time; or the gel should *not flow* under the action of a mechanical stress imposed for an infinite period of time. The former condition implies an infinite relaxation time t_R in a linear viscoelastic test while the latter stipulates the existence of a yield stress σ_y below which no flow occurs, i.e., below which the viscosity is infinite. Note that the stipulated conditions do not preclude relaxation or flow occurring at higher (nonlinear) stresses or strains.

The existence of gel-like rheological properties in a sample can be qualitatively diagnosed by simple ("tabletop") experimental tests without using a rheometer. Such tests, which rely on visual observation and feel, are particularly useful in evaluating the sol-gel boundary. In a typical study, samples are placed in a bath at constant temperature and their physical state (sol or gel) is noted, for instance, by tube inversion. The bath temperature is then varied and the samples are equilibrated at a new temperature, whereupon their physical state is again recorded. This process is repeated over the temperature range of interest. Alternately, instead of equilibration, a slow heating or cooling rate (e.g. $<1^\circ$/min) may be imposed. Through these studies, a plot of T_{gel} versus gelator concentration c can be obtained.

We consider below some of the common "tabletop" tests for gelation that have a rheological basis. A discussion of gelation and gel point based on standard rheological measurements (using a rheometer) is given in Chapters 5, 6, and 19.

2.1. Tube Inversion

The most common diagnostic test of gelation is to turn a test-tube or vial containing the sample upside-down and then to note whether the sample flows under its own weight (Figure 1). It is assumed that a sample having a yield stress (gel) will not flow whereas a viscous but inelastic sample (sol) will show appreciable flow [3]. The simplicity of this test makes it the method of choice in phase behavior studies with molecular gels.

Care must be taken in conducting and interpreting tube inversion experiments. It is easy to mistake a viscous sol for a gel and conversely, to misinterpret a gel with a small yield stress to be a sol. To understand why, we will consider the basis for the tube inversion test. Before doing so, it is useful to recall that the yield stress σ_y is given by [3]:

$$\sigma_y = G \cdot \gamma_c \tag{1}$$

where G is the gel modulus and γ_c is the critical strain that marks the linear viscoelastic limit (critical strain at yield). The gel modulus signifies the stiffness or rigidity of the network, while the critical strain denotes the strength of bonds in the network. Thus, for σ_y to be high, both G and γ_c should be high.

In the tube inversion test, consider a sample with yield stress σ_y placed in a cylindrical vial of radius R, with the length of the vertical column of sample being L (Figure 1b). The sample mass is $\pi R^2 L \cdot \rho g$, where ρ is the sample density and g the acceleration due to gravity. The condition for static equilibrium, from the von Mises yield criterion, balances the yield stress with the gravitational stress [4]:

$$\sigma_y \cong \rho g \cdot L \tag{2}$$

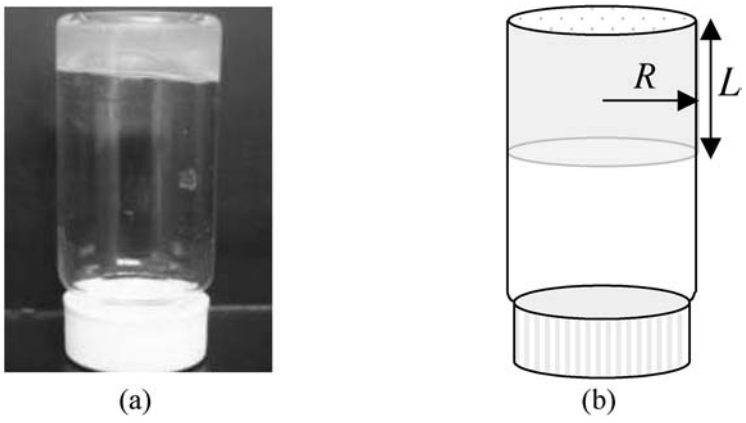

Figure 1. (a) Photograph of a gel from the author's lab that satisfies the tube inversion test; (b) The test sample is idealized as a cylinder of radius R and length L.

It is assumed here that the sample yield coincides with the disruption of the network structure in the gel.

Equation (2) shows that the tube inversion test is dependent on both sample mass and vial size. The column height L is proportional to sample mass and density, and inversely related to vial size for a given mass. When using this test for phase behavior determination, it is therefore crucial to use the *same sample mass and vial type* (geometry, size).

Rheological tests can confirm the approximate yield stress values indicated by tube inversion. For example, Booth *et al.* [5, 6] studied aqueous gels of block copolymers using both tube inversion and conventional rheometry. They used 0.5 g of each sample in tubes of 1 cm internal diameter. Under these conditions, samples of yield stress $\sigma_y \geq 40$ Pa were able to hold their own weight indefinitely. Incidentally, this value is in rough agreement with Eq. (2).

The time of observation can also influence the outcome of tube inversion experiments. To understand this, consider how a highly viscous but inelastic sample would behave in the same inverted geometry as in Figure 1b. In this case, the sample would move (flow) downward by a distance ε over a time t under the action of gravity. An approximate expression for ε is obtained by balancing the gravitational and viscous stresses [4]:

$$\frac{\varepsilon}{t} \cong \frac{\rho g L R}{\eta} \tag{3}$$

Here, it is assumed that the sample viscosity η is invariant with shear-rate. This equation shows that a high viscosity can inhibit motion of the sample. Using a high value of η, say 10^5 Pa.s (a very reasonable value for a pre-gel) together with typical geometry conditions suggests that a sample may move only a few millimeters in a couple of minutes. Thus, based on a short period of observation, the motion detected may be so negligible that one may erroneously classify the sample as a gel. To prevent such mistakes, a sufficiently large observation time must be employed in tube inversion experiments. Experiments with a test fluid such as honey (a highly viscous but inelastic fluid) may be used to gauge timescales with viscous fluids and thereby to "calibrate" the geometry of choice.

2.2. Falling of Spheres

A second method used for determining the onset of gelation is to examine the motion of small spherical particles suspended in the sample (Figure 2). This method is an adaptation of the Stokes' law problem to yield stress fluids. A quantitative criterion has been derived by Beris *et al.* [7] assuming that the fluid can be approximated as a Bingham fluid (i.e., no flow till the yield stress; Newtonian flow at higher shear stresses). Their prediction is that a spherical

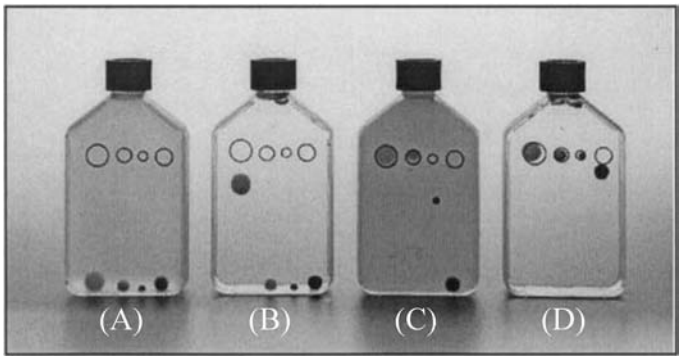

Figure 2. Photograph of the falling sphere test in a series of viscoelastic or gel-like fluids. The circles show the initial position of the test spheres, whereas this photograph was taken after one month of storage. The four spheres in each flask correspond to different sizes and densities: the furthest to the left is a low-density plastic sphere, while that at the rightmost is made of high density steel. The four samples are aqueous solutions of: (A) 2.1% guar gum; (B) 2.3% carboxymethyl cellulose; (C) 6% Xanthan gum; (D) 0.4% Carbopol® 940F. Reproduced with permission from Ref. [8] (copyright Noveon Inc.).

ball of size R_b and density ρ_b will not fall in a fluid of density ρ and yield stress σ_y provided [4, 7]:

$$\sigma_y > 0.095(\rho_b - \rho)g \cdot R_b \tag{4}$$

It is clear from Eq. (4) that the particle size and density dictate the balance between gravitational stress and the yield stress. This intuitive picture is illustrated by Figure 2 where the settling of spheres of different sizes and densities is shown in a range of viscoelastic polymeric fluids [8]. The Xanthan gum and Carbopol® samples are physical gels that have appreciable yield stresses and hence are able to suspend dense spherical particles for more than a month [8].

In using sphere settling for characterizing molecular gels, the ideal scenario is for the sphere to remain immobile in the gel phase, but to rapidly settle in the sol phase. For this, it is preferable to use a dense ball, e.g. of steel or other metal, that is also sufficiently large. An important precaution is that the sample tube or vessel should be much larger than the test sphere – if this is not so, the presence of nearby walls can influence the motion of the sphere [9]. However, eliminating wall effects completely would require an impractically large amount of sample, so a compromise between accuracy and process economics has to be reached. Finally, it is also important that the sphere settle from rest – most gels tend to be shear thinning fluids and if the sphere is dropped into the fluid with a force, the fluid in the local vicinity may be thinned, thus promoting further downward motion of the sphere [9]. A simple way to ensure settling from rest is to place a dense ball *on top* of the gelled material within a sealed vial [10].

2.3. Rise of Bubbles

A third method for evaluating the gel-like nature of a sample is to observe the motion of bubbles in a sample. Bubbles can either be injected specifically for this test or they may remain in the sample after preparation. The essential idea is that bubbles will remain trapped in a gel whereas they will slowly rise to the surface in a viscous fluid [11]. Note that the bubble rise problem is mathematically identical to the settling sphere problem in Newtonian fluids and thus, the rise velocity is expected to inversely scale with the fluid viscosity. Therefore, to distinguish between a viscous sol and a gel requires long periods of observation.

Bubble rise may still be a useful test for certain gels. When a sample is heated, the bubbles tend to rise faster. Thus, for gels that form only upon heating, the trapping of bubbles may provide a stark contrast between sols and gels. Likewise, techniques that are used to remove bubbles can serve as a "quick and dirty" rheological indicator. For example, if gel samples are routinely centrifuged to remove bubbles, then the persistence of bubbles after various extents of centrifuging (speed and duration) may offer a rapid qualitative gauge of both the sol-gel boundary as well as the variation of yield stress or gel modulus among different samples.

2.4. Other Methods

In principle, any method used to measure the yield stress can also be used to devise a rheological criterion for gelation. The rheological literature reports several inexpensive approaches to measure yield stress, most of which are variations on the themes explored above. For example, instead of tube inversion, it is also possible to use an inclined plane, with the yield stress correlating with the thickness up to which the sample stays intact on the plane [12].

A further variation on the inverted tube removes the influence of the container walls [4]. Here, a sample is *extruded* through a tube (Figure 3), exposing a piece of gel to gravitational tension. The maximum length $L_{\max}$ at which the gel fractures can be correlated to the yield stress, in a manner analogous to Eq. (2), as long as $L_{\max}$ greatly exceeds the radius of the tube. Figure 3 shows a demonstration of this test with a yogurt gel.

Finally, Boger *et al.* [13] also showed how to develop a "50 c rheometer" by utilizing the **slump test**. This method was originally used to determine the flow properties of fresh concrete. Here, a cylindrical frustum is filled with the sample and then the frustum is lifted off, allowing the sample to collapse under its own weight. The difference between the initial and final heights (i.e., the slump height) is inversely related to the yield stress.

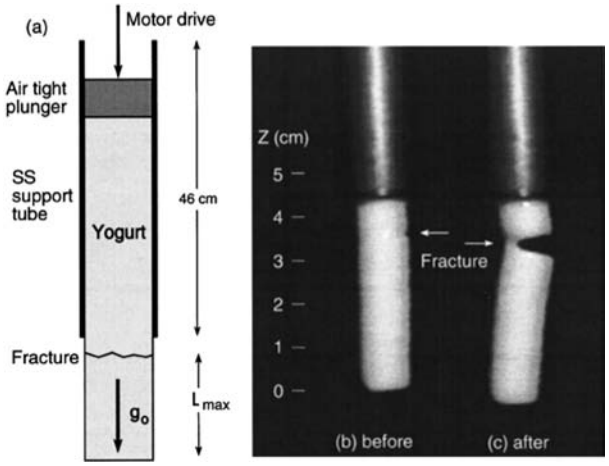

Figure 3. Extrusion of gel (yogurt) cylinders to measure their yield strength. A schematic of the configuration used is shown in (a). When the extruded length exceeds $L_{\max}$, the gel fractures. Images taken (b) before and (c) after fracture of the sample are also shown. Reproduced with permission from Ref. [4] (copyright American Institute of Physics).

3. Thermodynamics of Gelation: Sol-Gel Transition by Calorimetry

A second approach for constructing gelator phase diagrams is using thermal characterization techniques such as differential scanning calorimetry (DSC). Before we discuss this topic further, it is useful to briefly review the thermodynamics of gelation. The same topic is discussed in much more detail in Chapter 1.

3.1. First- and Second-Order Phase Transitions

Is the sol-gel transition a first- or second-order process? There have been many conflicting views on this issue, and we mention only the key points here. First, let us distinguish between these two types of transitions [14].

First-order transitions are sharply defined – all molecules undergo the transition in unison, provided there is sufficient thermal energy. Thus, quantities that are first derivatives of the chemical potential μ, such as the enthalpy H and specific volume V, change discontinuously at the transition. Second derivatives of μ like the heat capacity c_p (i.e., $\mathrm{d}H/\mathrm{d}T$) show a singularity (i.e., the system has an infinite heat capacity at the transition temperature). First order transitions typically proceed by a *nucleation and growth* mechanism and hence often exhibit metastabilities arising from supercooling or superheating.

Second-order transitions, on the other hand, are "smooth". The enthalpy H and specific volume V change continuously, while the heat capacity c_p shows a discontinuity. In such transitions, the molecules begin to undergo changes well before the transition temperature. The transition tends to be co-operative (i.e., groups of molecules act in accord). As the transition point is approached, the range of co-operativity increases, and this range or "domain size" diverges at the critical point. Many properties of the system diverge through power laws with respect to the distance from the critical point T_c (i.e., *property* $\sim (T - T_c)^{\beta}$). Second-order transitions occur by *spinodal decomposition* in the unstable or spinodal region of the phase diagram. Between the binodal and spinodal curves, the system phase separates via nucleation and growth, thus allowing metastabilities to occur.

3.2. The Question of Gelation

In a DSC scan (Figure 4), the process of molecular gelation upon cooling is often associated with an exothermic peak. Conversely, the process of gel melting or dissolution upon heating is associated with an endothermic peak. A *sharp* calorimetric peak indicates a *discontinuous* enthalpy change, implying that the transition is first order. Guenet, in his book on polymer and biopolymer gels [15], states that "in most cases, gel formation proceeds via a first-order transition". Note that the melting transition alluded to here does not correspond to the melting point of the gelator itself – the latter typically occurs at much higher temperatures.

The melting peak for gelation, however, is often rather broad [5] or even absent [17], suggesting that the transition may be weakly first-order or possibly second-order. Support for the latter viewpoint arises from the power law dependence of rheological properties in the vicinity of the gel point. Such power laws also lend support to the idea of gelation as a percolative process [1]. Percolation theory assumes that the gelator molecules assemble first into small clusters, which then further assemble into a three-dimensional (3-D) volume-filling network. Thus, the cluster size or correlation length increases in a power law as the gel point is approached. The divergence of the correlation length is characteristic of a second-order process.

In the case of molecular gels, the experimental data can be rationalized in the following manner [18]. It is assumed that the gelator molecules assemble into fibrils, strands, ropes or other assemblies by a first-order process (i.e., with a discontinuous enthalpy change). These assemblies then further link together to form clusters and ultimately the network structure. The cluster size diverges, as in a second-order transition.

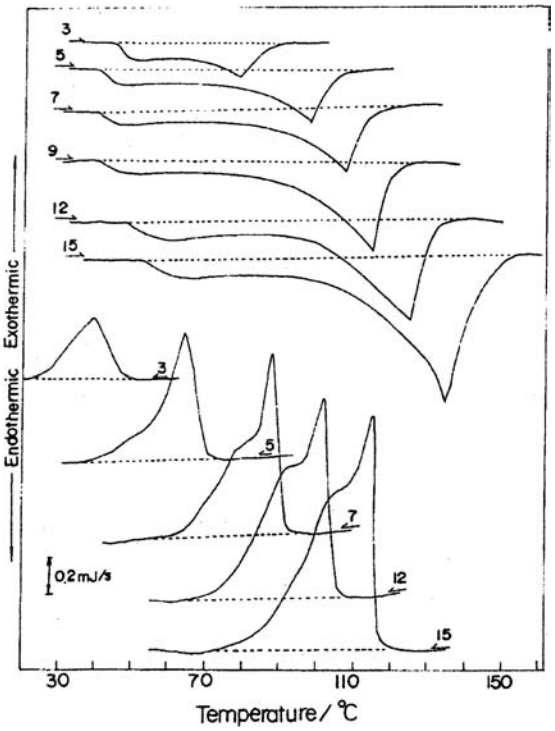

Figure 4. DSC curves (heating, bottom and cooling, top) for the gelator dibenzylidene sorbitol (DBS) in triethylene glycol. The numbers represent the gelator concentration in w/w. The dashed lines are baselines used for the calculation of enthalpies. Reproduced with permission from Ref. [16] (copyright American Chemical Society).

3.3. Calorimetry of the Sol-Gel Transition

In DSC, a sample cell and a reference cell are maintained at the same temperature. The power supplied to raise the temperature of each cell at a constant rate (e.g. 10° C/min) is recorded. This power is converted to a heat capacity vs. temperature curve. The peak temperature in a heating curve corresponds to the gel "melting" point T_{gel} and the area under the peak yields the enthalpy of gelation (melting). Figure 4 shows DSC curves for a sorbitol-based molecular gelator in an organic solvent [16]. As the gelator concentration is increased, both the melting temperature and the enthalpy of melting are observed to increase. Note that there is some hysteresis in the gelation behavior, with the gel-to-sol transition (melting) not coinciding perfectly with the sol-to-gel transition. Also the peak is better defined in cooling curves rather than in heating curves.

3.4. Gelation Temperature vs. Gelator Concentration

Plots of the gelation temperature T_{gel} vs. gelator concentration c are shown in Figure 5a for a sugar-based gelator in two organic solvents [19]. Note that there is an exponential increase of c with T_{gel}. In turn this implies that an Arrhenius plot of ln c vs. $1/T_{gel}$ will be linear, and this is nicely confirmed by Figure 5b.

The above experimental result for T_{gel} vs. c is well established for a wide range of gelators, both molecular, as well as polymeric. However, its physical implication is still controversial. There are at least two models that can explain such a relationship. First, the gel-to-sol transition can be interpreted as a melting or dissolution of gelator *crystals* [14]. In that case, the gelator concentration corresponds to the solubility of its crystals in an ideal solution at a temperature T_{gel} and is given by the following equation [1, 19]:

$$\ln c = -\frac{\Delta H_m}{RT_{gel}} + \text{constant} \tag{5}$$

where R is the universal gas constant and ΔH_m is the enthalpy of fusion (melting) of the neat gelator. The above equation has been referred to as Schrader's equation [19] or the Schroeder-van Laar equation [17]. Note that this assumes that the transition is first order. Eliminating the constant from Eq. (5) gives:

$$\ln c = -\frac{\Delta H_m}{R}\left(\frac{1}{T_{gel}} - \frac{1}{T_m}\right) \tag{6}$$

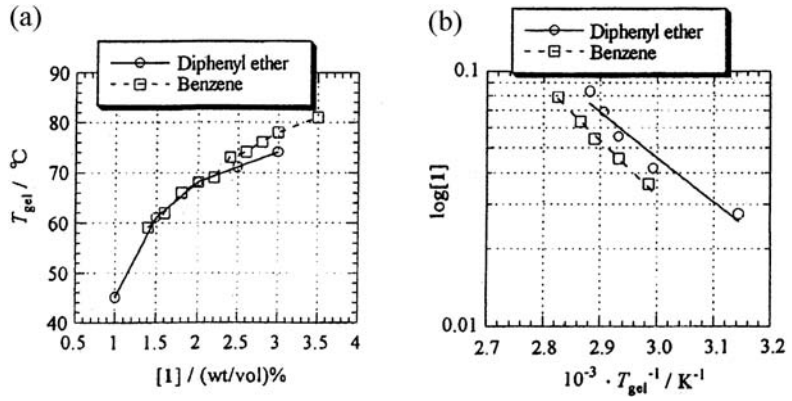

Figure 5. (a) Sol-gel phase boundaries for dibenzylidene sorbitol (DBS) in two organic solvents determined by tube inversion. (b) The same data plotted in an Arrhenius-type plot. Reproduced with permission from Ref. [19] (copyright Royal Society of Chemistry).

Here T_m is the melting temperature. Values of ΔH_m obtained via Eq. (6) are typically comparable or slightly higher than values from DSC measurements at the melting point of the gelator [19].

An identical form of Eq. (5) can be derived from very different assumptions. Eldridge and Ferry [20] assumed that the gelation of biopolymers, such as gelatin, is controlled by a pairwise crosslinking of biopolymer chains. The crosslinking reaction is exothermic, and therefore one can write:

$$\ln c = \frac{\Delta H_{\mathrm{cr}}}{RT_{\mathrm{gel}}} + \text{constant} \tag{7}$$

Here, ΔH_{cr} is the heat evolved in the crosslinking reaction. Once again, this equation suggests an Arrhenius relationship from which one can obtain ΔH_{cr}. Note, however, that gelation is considered here to be a second-order process, which is in direct contrast to the assumptions inherent in Eq. (5).

4. Conclusions and Perspectives

In this chapter, we have described how the *phase diagram* for molecular gelators can be obtained using simple, straightforward techniques. The phase diagram is a plot of temperature vs. gelator concentration showing the location of sol-gel boundari(es) as well as any multi-phase or lyotropic regions. The first set of techniques involve application of rheological principles to detect gelation. These include: (a) tube inversion; (b) falling sphere; and (c) rising bubbles. Calorimetry studies are also useful in directly measuring the enthalpy of gelation (melting). The latter quantity can also be obtained by analyzing an Arrhenius plot of the gelator concentration as a function of the gelation temperature.

Among the rheology-based methods, tube inversion is by far the most popular and convenient, and arguably also the least ambiguous. As a starting point for studying gels, it is preferable to use tube inversion over falling ball or other alternatives. If falling ball must be used, it is important to use a heavy ball and a sufficiently large vessel in order to obtain a clean measurement. Finally, where possible, the simple "tabletop" rheological methods should be benchmarked using data from conventional rheometry.

References

[1] Terech, P.; Weiss, R.G. *Chem. Rev.*, **1997**, *97*, 3133–3159.
[2] Winter, H.H. "Gels", In *Encyclopedia of Polymer Science and Engineering*, H.H. Mark, Ed., New York: Wiley, **1985**, pp. 343.
[3] Macosko, C.W. *Rheology: Principles, Measurements and Applications*, New York: VCH Publishers, **1994**.

[4] Dimonte, G.; Nelson, D.; Weaver, S.; Schneider, M.; Flower-Maudlin, E.; Gore, R.; Baumgardner, J.R.; Sahota, M.S. *J. Rheol.*, **1998**, *42*, 727–742.
[5] Li, H.; Yu, G.E.; Price, C.; Booth, C.; Hecht, E.; Hoffmann, H. *Macromolecules*, **1997**, *30*, 1347–1354.
[6] Kelarakis, A.; Mingvanish, W.; Daniel, C.; Li, H.; Havredaki, V.; Booth, C.; Hamley, I.W.; Ryan, A. J. *Phys. Chem. Chem. Phys.*, **2000**, *2*, 2755–2763.
[7] Beris, A.N.; Tsamopoulos, J.A.; Armstrong, R.C.; Brown, R. A. *J. Fluid Mech.*, **1985**, *158*, 219–244.
[8] Noveon, Inc. http://www.pharma.noveoninc.com/literature/bulletin/epb12.pdf "Bulletin 12: Flow and suspension properties", 2000.
[9] Gheissary, G.; van den Brule, B.J. *Non-Newtonian. Fluid Mech.*, **1996**, *67*, 1–18.
[10] van Esch, J.; Schoonbeek, F.; de Loos, M.; Kooijman, H.; Spek, A.L.; Kellogg, R.M.; Feringa, B.L. *Chem.-Eur. J.*, **1999**, *5*, 937–950.
[11] Stein, S.; Buggisch, H.Z. *Angew. Math. Mech.*, **2000**, *80*, 827–834.
[12] Coussot, P.; Boyer, S. *Rheol. Acta*, **1995**, *34*, 534–543.
[13] Pashias, N.; Boger, D.V.; Summers, J.; Glenister, D.J. *J. Rheol.*, **1996**, *40*, 1179–1189.
[14] Atkins, P.W. *Physical Chemistry*, 5th edition, New York: W.H. Freeman & Co., **1994**.
[15] Guenet, J.-M., Ed., *Thermoreversible Gelation of Polymers and Biopolymers*, London: Academic Press, **1992**.
[16] Watase, M.; Nakatani, Y.; Itagaki, H. *J. Phys. Chem. B*, **1999**, *103*, 2366–2373.
[17] Menger, F.M.; Caran, K.L. *J. Am. Chem. Soc.*, **2000**, *122*, 11679–11691.
[18] Terech, P.; Rossat, C.; Volino, F. *J. Colloid Interface Sci.*, **2000**, *227*, 363–370.
[19] Amanokura, N.; Yoza, K.; Shinmori, H.; Shinkai, S.; Reinhoudt, D.N. *J. Chem. Soc. Perkin Trans.*, **1998**, *2*, 2585–2591.
[20] Eldridge, J.E.; Ferry, J.D. *J. Phys. Chem.*, **1954**, *58*, 992–995.